Received: 29 July 2023 | Revised: 17 September 2023 | Accepted: 19 September 2023

DOI: 10.1002/pen.26519

RESEARCH ARTICLE

POLYMER ENGINEERING AND SCIENCE WILEY

Optimal design and operation of reactive extrusion processes: Application to the production and scale-up of polyurethane rheology modifiers for paints

Maximilian Cegla[1] | **Aleksandra Fage**[2] | **Simon Kemmerling**[2] | **Sebastian Engell**[1]

[1]Biochemical and Chemical Engineering Department, TU Dortmund University, Dortmund, Germany

[2]Fraunhofer Institute for Chemical Technology ICT, Pfinztal, Germany

Correspondence
Maximilian Cegla, Biochemical and Chemical Engineering Department, TU Dortmund University, Emil-Figge-Str. 70, 44227 Dortmund, Germany.
Email: maximilian.cegla@tu-dortmund.de

Funding information
EU Horizon 2020 SIMPLIFY, Grant/Award Number: 820716

Abstract

In this work, the methodology for the optimal design, operation and scale-up of reactive extrusion processes in twin-screw extruders previously presented in Reference (Cegla and Engell, 2023). is applied to the production of hydrophobically ethoxylated urethanes (HEURs). The new process is a promising alternative to the current batch technology in large reactors with long residence times. We demonstrate the use of model-based design and scale-up for this case. A novel mechanistic finite volume twin-screw extruder model is used as the process model, which is adapted to the process at hand by embedding a detailed description of the HEUR chemistry and rheology. An economic cost function is used to examine the scale-up process from an 18 mm extruder to a 27 and 75 mm extruders, considering a selected range of products. The comparison between the optimization results obtained for the individual products with the optimization results for the production of multiple material grades using the same screw setup shows the high flexibility of the extruder-based process. Significant energy savings compared with the conventional batch process can be achieved using reactive extrusion. To quantify the effort for the transition to a purely continuous production in terms of flexibility and process logistics, product changeovers are investigated.

Highlights

- Intensification of the HEUR production by reactive extrusion.
- Detailed model for the twin-screw extruder and the chemistry.
- Optimization of extruder, screw design, and operating conditions.
- Model-based scale-up from laboratory to industrial scale.
- Investigation of flexible industrial production of different HEURs.

KEYWORDS

extrusion, modeling, polyurethanes, reactive extrusion, simulations

1 | INTRODUCTION

Worldwide, 43 million tons of paints and coatings were produced in 2021.[1] In case of the waterborne systems, the desired spreading performance during application is adjusted by additions of rheological modifiers,[2] which typically, constitute up to 5% of the overall product formulation. Most common thickeners used in paints are functionalized additives, based hydroxyethyl cellulose, alkali-soluble emulsion, or ethoxylated urethanes.[3] Due to the structural and functional versatility of the hydrophobically modified ethoxylated urethanes (HEURs), they are currently most in-demand specialty paint additives in terms of production volume.[4] To produce these HEURs, an oligomeric diol, here poly(ethylene glycol) (PEG), is reacted with a diisocyanate (ISO) to generate a viscous hydrophilic backbone. This backbone is end-capped with a hydrophobic alcohol. As the thickening behavior of HEUR in a paint formulation is induced by the physical interactions of the hydrophobic tails, their performance can be tuned by the varying the chain length of hydrophilic core, as well as the end-capping alcohol.[5] Industrial production of HEURs is usually performed in batch reactors with a volume of several cubic meters, adding all reactants simultaneously, in a so-called one-step process. This leads to a broad molecular weight distribution, which is not advantageous for the product properties,[6] and the maximum molecular weight is limited by the processing capabilities of the stirring equipment. After the reaction is finished, the HEUR is formulated with water to clean the reactor and transport the product.

In the European project SIMPLIFY,[7,8] the transfer of this process to a continuous and fully electrified production using a corotating twin-screw extruder has been investigated. This transition offers numerous benefits in terms of process control, product quality, and cost-efficiency. Continuous production eliminates the energetically inefficient steps typical for a batch system, such as long production cycles, which additionally require cleaning of the reactor between every charge. Moreover, the use of a twin-screw extruder enables the production of new and more viscous products by a two-step process and reduces the quantities of hazardous ISO that are present in the apparatus.[9,10] In contrast to the work of Wolosz et al.[11,12] that employs reactive extrusion for the investigation of new isocyanate-free synthesis routes for HEURs in a laboratory scale, this work concerns a commercial product and its production at pilot and industrial scale. For the development of the novel continuous process, the model and optimization algorithm presented previously[13] is used. The model-based optimization reduces the required number of experiments. This is especially important as wide range of HEUR grades exists to satisfy the specific customer requirements[14] and not all of these can be extensively investigated for the necessary adjustment of the production conditions. The model-based optimization further enables an extrapolation from lab-scale extrusion synthesis to larger scale production equipment. The model consists of two parts, an accurate description of the extruder with the internal flows and a description of the rheological and chemical system. The extruder model is based on finite volumes as proposed by Eitzlmayr et al.[15] and has been adapted to reactive extrusion. For the optimization, a memetic algorithm which is a combination of an evolutionary strategy with a local gradient-based search is applied. The modeling approach and the optimization method were presented in Ref. 13 The parametrization of the extruder model enables a straightforward scale-up. Typically, the scale-up of extrusion processes is performed by keeping certain indicators constant, such as in the approach of scale-independent optimization strategy (SIOS). According to SIOS, the optimal operating point of the extrusion process is determined experimentally by adjusting the throughput and the speed of rotation, until the maximum conveying capacity of the extruder is reached, while maintaining good product quality.[16,17] However, the authors of Ref. 18 showed that after scale-up, the optimal configuration and operating parameters may lead to significant deviations in the residence time or in the specific energy consumption on the different scales. Keeping these indicators constant in a scale-up strategy would consequently lead to a suboptimal or potentially infeasible process. Therefore, simple scale-up approaches based on similarities are unreliable, especially for very complex processes such as reactive extrusion. In the work of Berzin et al.,[18] the viable solution space is determined based on response surfaces for the different operation parameters during scale-up. Drawback of the method is that during optimization, the optimal processing conditions for one screw configuration are determined, and in a second step these conditions are used during the optimization of the screw configuration itself, leading to suboptimal solutions.

In our work, the scale-up is performed based on the optimization of an economic cost function for the different equipment sizes and products. The proposed model-based scale-up also allows the investigation of the extruder length (length to diameter ratio) on the process performance, which is, besides the screw diameter, the second key characteristic of the extruder and essential for production planning.

2 | MATERIALS AND METHODS

2.1 | Extruder model

The established dynamic extruder model is based on the work of Eitzlmayr et al.[19] which has been extended for

the case of reactive extrusion. This model is presented in detail in Ref. 13 Figure 1 shows the discretization of the extruder into finite volumes of certain length with conveying and pressure driven flows between each element.

The overall flows between the elements depend on the local screw geometry, rotation speed, and pressure difference, as well as on the density and viscosity of the material. To accurately describe the internal melt flows, fluxes in both directions are considered using the backflow cell methodology. By this extension, it is possible to accurately describe the residence time distribution characteristics of the screw elements in the simulation of an extruder.[20] The pressure is modeled as a differential state in order to have a fixed model structure for optimization. The model is completed by the component balance equations that involve the local flows, concentrations, and the contribution of the chemical reactions. The local concentrations are used to determine the melt properties, such as the viscosity as function of the conversion. For each element, the heat balance is solved with contributions of convection, heat conduction, heat transfer between barrel and melt and of the dissipation of mechanical energy. To compute the steady-state behavior, the model is simulated for a sufficiently long-time horizon. Typically, the lengths of extruders are characterized by the length-to-diameter ratio (L/D) which can be increased by multiples of 4 up to 60. The length of an extruder block with an independent heating and cooling system is typically 4 L/D. For optimization, four types of Leistritz Maxx twin-screw extruders are considered in this work: (1) 18 mm bench scale with L/D = 60, (2) 27 mm pilot scale with L/D = 44, (3) 75 mm industrial scale with L/D = 40, and (4) 75 mm industrial scale with L/D = 60. The parametrization of the extruders is given in Table 1. The centerline distance describes the distance between the centers of the two screws.

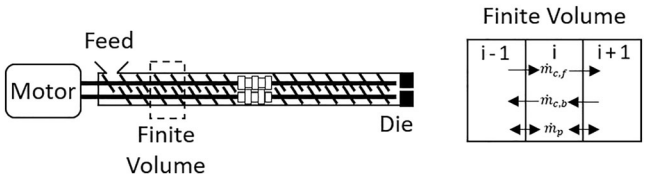

FIGURE 1 Schematic of the extruder discretized into finite volumes.

2.2 | Chemical model of the HEUR system in reactive extrusion

Our case study examines the production of hydrophobically modified ethoxylated polyurethane (HEUR) thickeners, performed in the extruder in a two-step approach. As shown in Figure 2, the initial zones of the extruder are used for the chain growth of the polymer backbone, while chain termination is executed in the further sections of the barrel. From the chemical perspective, the chain growth step yields an isocyanate-terminated prepolymer, obtained by coupling of PEG, with a weight average molar mass (M_w) of 8000 g/mol, and an aliphatic ISO used in molar excess. As the ISO, 4,4′-Methylenebis (cyclohexyl isocyanate) was used in this study. The maximum molecular weight $M_{w,max}$ for the given stoichiometric ratio of PEG and ISO, can be reached by promoting a sufficiently fast progress of the reaction through the adjustment of the melt temperature and by ensuring the required reaction time through setting of the

Parameter	18 mm	27 mm	75 mm	75 mm
D screw diameter (mm)	18.5	28.3	77.0	77.0
D_C screw core diameter (mm)	11.2	17	46.4	46.4
C_L centerline distance (mm)	15	23	61.5	61.5
L/D length/diameter ratio (−)	60	44	40	60
L screw length (m)	1.1	1.2	3.0	4.5

TABLE 1 Geometrical parameters of the Leistritz 18 mm Maxx, the Leistritz 27 mm Maxx, and the Leistritz 75 mm Maxx extruders.

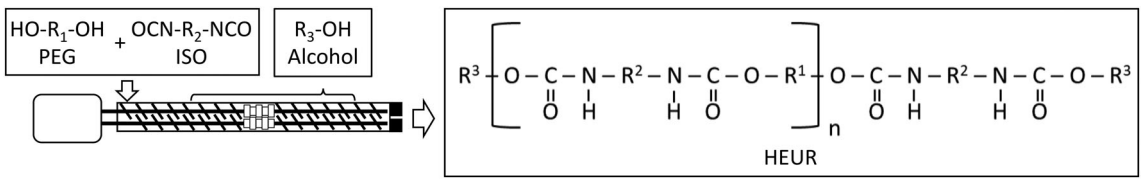

FIGURE 2 Composition of the hydrophobically ethoxylated urethane polymer molecule of length n. R^1 is the residual of poly(ethylene glycol), R^2 is the residual of the diisocyanate, and R^3 is the residual of the alcohol.

parameters that influence the residence time in the extruder. The chain termination step is achieved by subsequent addition of a hydrophobic alcohol (1-octanol) at a selected position in the extruder which then end-caps the prepolymer. The correct stoichiometric ratio between the reactants is crucial to control the molar mass of the HEUR species and to form the double-end-capped structure which are the basic factors that determine the thickening efficiency of the product.

The reaction kinetics of this step-growth polymerization[21] are modeled by a differential equation for M_w, similar to,[22] which is extended by a term for the chain termination by the reacted alcohol A_r. In contrast to Ref. 23, $M_{w,max}$ is considered in the reaction kinetics. The parameter k_{ct} quantifies the effect of the reacted alcohol on $M_{w,max}$. Effects of side reactions that occur for polyurethanes (PU) are not relevant in the given temperature range for the investigated residence times.[24] We therefore propose to describe the reaction system by:

$$\frac{dM_w}{dt} = k_{0,cg} \cdot \exp\left(\frac{-E_{A,cg}}{RT}\right) \cdot \left|\frac{M_{w,max} - M_w[A_r] \cdot k_{ct}}{M_{w,max} - [A_r] \cdot k_{ct}}\right| \quad (1)$$

$$\frac{d[A]}{dt} = -\frac{d[A_r]}{dt} = [A] \cdot \left(\frac{2M_{w,rep}}{M_w} - [A_r]\right) \cdot k_{0,ct} \cdot \exp\left(\frac{-E_{A,ct}}{RT}\right) \quad (2)$$

The melt behaves quasi-Newtonian. The influence of the temperature on the viscosity is described by an Arrhenius approach, while the influence of the molecular weight is described by a power law. The exponent 3.4 is reported in the literature as being valid for linear polymers like polyurethanes.[22,25] Consequently, the viscosity is described by:

$$\eta(T, M_w) = \eta_0 \cdot M_w^{3.4} \cdot \exp\left(\frac{-E_{A,eta}}{RT}\right). \quad (3)$$

Within this work, the ratio between PEG and ISO is kept constant at a molar ratio 1:1.3, which corresponds to a $M_{w,max}$ of 60 kg/mol. A preliminary investigation of the processing parameters, which are suitable for synthesis of HEUR by reactive extrusion was performed using a laboratory scale Thermo Scientific HAAKE MiniLab II micro compounder with a capacity of 7 g. As the micro compounder has a built-in by-pass capillary, which circulates the material, it is possible to monitor the chain growth via the melt viscosity, calculated based on the pressure drop over the capillary. A recycle extruder was used to determine the reaction kinetics as it has a similar pre-mixing and mixing performance of the reactants as the pilot-scale process and a larger reaction volume compared with a plate-cone viscometer. To determine the kinetics of chain growth, the first reaction step (PEG + ISO) was carried out at two temperature settings, yielding the viscosity profiles shown in Figure 3. The intersection of the two viscosity curves emphasizes the importance of modeling both influences of the temperature: on the reaction rate and on the melt viscosity. Subsequent experiments showed that the evolution of the molecular weight in the chain growth step can be limited by chain termination, induced by the addition of alcohol ([PEG + ISO] + alcohol) at a specific reaction time into the feed port of the recycle extruder. In a continuous process, this corresponds to selecting the appropriate dosing port along the barrel for the injection of the alcohol. Additional to the viscosity measurements, Fourier-transform infrared spectroscopy (FTIR) and size-exclusive chromatography measurements were carried out to determine the ISO conversion and the molecular weight of the polymer. Whereas diffusion limitations are observed in the batch setups, in reactive extrusion full ISO conversion (unreacted ISO below the limit of detection) was achieved and no limitations by diffusion effects were observed. This is explained by the significantly better mixing in a smaller volume for reactive extrusion, at also higher temperatures, lower viscosities, and shorter residence times. No production of side products, for example, allophanate was observed, as determined by the FTIR measurements.

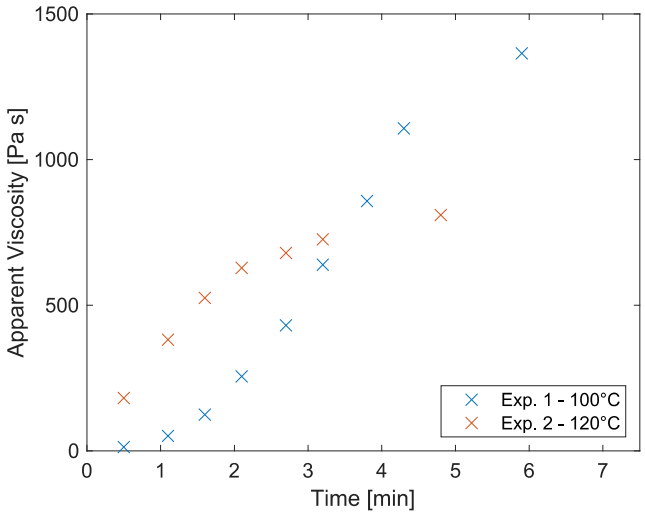

FIGURE 3 Measured evolution of the viscosity for the determination of the reaction kinetics in the HAAKE MiniLab II for experiments at 100 and 120°C.

The value of $M_{w,max}$ can be reduced by blocking of the chain growth by an excess of alcohol. In industrial practice, such control over the targeted molecular weight of HEUR is achieved by adjustment of the stoichiometry between PEG, ISO, and alcohol to ensure the desired molecular architecture. To reflect this, the model can subsequently be enlarged with additional degrees of

freedom that are required by the specific chemical system. Within this work, the feed of PEG and ISO is kept at a fixed molar ratio 1:1.3, which corresponds to a $M_{w,max}$ of 60 kg/mol, while the ratio of PEG and alcohol is varied between 1:0.60 and 0.72 to modulate the targeted molecular weight of the product. The proposed reaction kinetics in Equations (1) and (2) showed a good accordance with the experimental results. For the heat capacity (2.5 kJ/kg K), thermal conductivity (0.23 W/[mK]), and density (1125 kg/m^3) of the reaction mixture the values of pure PEG ($M_w = 8000$ g/mol) are assumed as it is the main component with >95 wt.%.[26] The heat of reaction for such a PU-system is negligible.[22] The parameters of the chemical and rheological models are presented in Table 2.

2.3 | Optimization of the production process

For the optimization of the reactive extrusion process, the memetic algorithm described in Ref. 13 is applied. This optimization method is a combination of an evolutionary algorithm (EA) that has already been successfully applied for the screw design optimization[27,28] and a local gradient-based optimization. The local optimization is performed to reduce the optimization time by reducing the search space of the EA and speeding up the search for local optima. This is important since the more detailed process model leads to larger computation times per model evaluation. By including a local optimization, a very accurate model can be employed which increases the reliability of the results. Common cost functions used in design optimization in the chemical industry focus on economic considerations, such as the maximization of revenues or net present value. A simple economic goal in this case is to maximize the throughput, assuming that the energy costs are significantly smaller than the product revenue and there is sufficient demand for the product:

$$\min -\dot{m} \tag{4}$$

This leads to the minimization of the fixed costs per mass of produced product, such as salaries, depreciation, or amortization. As an alternative, a cost function can be considered that also takes into account the energy demand of the process per mass of product:

$$\min \frac{\dot{Q}}{\dot{m}} \tag{5}$$

The energy is introduced into the process by electrical energy for heating and for the electrical drive of the extruder. It is also possible to impose constraints of arbitrary complexity that are formulated in terms of the internal model variables, for example, maximum values of temperatures. The tradeoff between different types of costs can be described by more complex economic cost functions, for example, including a CO_2 price. This is computationally more efficient than a multi-objective optimization as proposed by Teixeira for multiple performance indicators such as mechanical strain and mechanical energy input.[29,30]

2.4 | Scale-up

As reported by Kohlgrüber,[31] the scale-up of twin-screw extruders in practice often relies on the use of similarity

TABLE 2 Parameters of the model of the HEUR reaction and of the rheological model.

Parameter	Description	Value	Unit
ΔH	Reaction enthalpy	0	J/g
$M_{w,max}$	Max. polymer molecular weight	6×10^4	g/mol
$M_{w,rep}$	Molecular weight repetition unit	8×10^3	g/mol
k_{ct}	Constant termination	1.73×10^5	1/s
$k_{0,cg}$	Rate constant growth	1.2×10^6	1/s
$k_{0,ct}$	Rate constant termination	6.77	1/s
$E_{A,cg}$	Activation energy growth	5.6×10^3	J/mol
$E_{A,ct}$	Activation energy termination	917	J/mol
R	Universal gas constant	8.314	−J/(mol K)
η_0	Reference viscosity	1.8×10^{-15}	Pa s/(g/mol)$^{3.4}$
$E_{A,eta}$	Activation energy viscosity	−2905	−J/mol

Abbreviation: HEUR, hydrophobically ethoxylated urethane.

relations between the different equipment sizes. An example for this approach is geometrically similar extruders, for which the number of flights of the screw elements and the ratio of core to flight diameter is constant. This is typically the case within the same product line of twin-screw extruders (e.g., Leistritz Maxx extruders). Energetic similarity is also often used and is quantified by the maximum allowed specific torque of the extruders. Alternatively, it can be aimed at keeping constant operating conditions such as shear rates, general screw configuration, discharge pressures, specific heating or residence times as reported in Ref. 32 In the past, also power law expressions were suggested which originate from single-screw extrusion, such as[33,34]:

$$\frac{X_1}{X_2} = \left(\frac{D_1}{D_2}\right)^x \tag{6}$$

where X_1 and X_2 indicate a quantity of interest (e.g., residence time, pressure, shear rate) for the current and the scaled-up extruder. The drawback of the similarity-based approach is that its performance depends on the choice of the relationship that is used for scale-up. Also, the use of such relationships reduces the solution space. Model-based optimization has a significantly larger potential, as the optimal processing conditions and configuration for larger equipment do not have to coincide with the optima for smaller equipment.[35]

Ortiz-Rodriguez and Tzoganakis[36] proposes the use of the thermal time[37] t_T as a metric for scaling up, which is computed from the residence time distribution, the temperature profile, and the activation energy E of the reaction:

$$t_T = \int_0^t e^{-E/RT(t')} dt' \tag{7}$$

To quantify the absolute reaction progress, t_T integrates the reaction rate dependent on temperature over the residence time. This concept was shown to be applicable to the case of the degradation of polypropylene in reactive extrusion.[36] However, it is not applicable in case of more complex reaction systems, as in those cases the reaction progress is additionally a function of the concentration profile, and the activation energies of all reactions have to be considered. Examples that were studied using the 1D-simulation tool Ludovic© are given in Refs. 18,38 Even though these approaches use process simulation, simulation is employed only to explore feasible regions of configurations and operating parameters rather than to optimize the process for a given objective function. Also, the complexity of the reaction system is limited by the solution strategy, and therefore not applicable to the HEUR system. The mechanistic twin-screw extruder model presented in Ref. 13, can take into account complex reaction systems. The model describes accurately the strong coupling between the operating conditions, such as the reaction temperature and the residence time. Therefore, with this model in combination with the proposed optimization strategy and different extruder parametrizations, a model-based scale-up can be performed. Extruders of different brands can be directly parametrized in the model by their geometric properties such as diameters, centerline distances, or screw core to outer diameter ratios.

3 | RESULTS

In the following, the optimization of the HEUR production is performed for the bench scale and subsequently scaled-up to pilot and production scale. The process model combines the extruder model (Section 2.1) and the model for the chemical system (Section 2.2). The EA summarized in Section 2.3 and presented in detail in Ref. 13 was applied with a population size of 20 individuals, an elite percentage of 20% and a probability of 0.25 for the inversion. The production of HEURs with different molecular weights is of interest for the industrial application, as it directly contributes to the thickening efficiency of the product. Therefore, three target product grades were defined with the following molecular weight ranges that are typical for HEUR thickeners: 45–50, 50–55, and 55–60 kg/mol. To account for the temperature effects of end-capping and chain growth, the barrel temperature of the extruder is set using two different temperature zones. The first zone comprises two third of the extruder length and the second zone the last third of the barrel length. This necessitates the adjustment in the cost function as shown in Section 2.3, as two barrel temperatures significantly increase the heat losses due to heat conduction. These losses are calculated by the barrel heat conduction in the cross-sectional barrel area A_{surf} over the distance Δx between the centers of two barrel elements with the thermal conductivity coefficient of steel λ_{steel} and the temperature difference ΔT. The energy demand for cooling is assumed as 10% of the total cooling energy as cooling can be provided by for example, cooling towers.

Thus the energy-related cost function for the HEUR case is:

$$\min \frac{\dot{Q}_{heat} + \dot{Q}_{mech} + 0.1 \cdot \dot{Q}_{cool}}{\dot{m}} + 1.1 \cdot \frac{\Delta T \cdot \lambda_{steel} \cdot A_{surf}}{\Delta x \cdot \dot{m}}. \tag{8}$$

Within the optimization, the sequence of the screw elements as well as the position of the alcohol feed is the

Parameter	Description	Unit	Type
S_{conf}	Screw configuration	—	Discrete
P_{feed}	Position alcohol feed	—	Discrete
n	Speed of rotation	rpm	Continuous
$\dot{m}$	Throughput	kg/h	Continuous
$T_{b,1}$	Barrel temperature first section	°C	Continuous
$T_{b,2}$	Barrel temperature second section	°C	Continuous

Abbreviation: HEUR, hydrophobically ethoxylated urethane.

TABLE 3 Overview of the optimization variables for the HEUR system.

Parameter	1	2	3	4	5–8	9	Die
Length (mm)	240	15	15	240	120	120	15
Element	R30	L20	R30	R30	R20	SME	Ø4 mm

Note: The positions of the underlined elements can be changed by the optimizer. R30 and L30 indicate forward and backward conveying elements with a pitch of 30 mm. The SME elements have a pitch of 20 mm. A round die of 15 mm length and 4 mm diameter is used.
Abbreviations: HEUR, hydrophobically ethoxylated urethane; SME, screw mixing element.

TABLE 4 Screw configurations for the bench scale HEUR case.

discrete decision variables. Additionally to the two barrel temperatures of the two sections, the overall throughput and the speed of rotation are considered as continuous decision variables. The optimization variables for the bench, pilot, and production scale HEUR production are summarized in Table 3.

3.1 | Optimization of the HEUR production in a bench scale extruder

The first investigated case for the bench scale production of HEUR is the design of an Leistritz 18 mm Maxx extruder with L/D = 60. The geometry of the extruder is presented in Table 1. This scale is optimal for R&D purposes, providing valuable insights into the technical aspects of the process at relatively low throughputs, thus reducing the costs of the reactants. Furthermore, this extruder size offers a high flexibility for rapid adjustments of the configuration, of the measurement strategy, as well as of the screw design.

The limitations imposed on the optimization are a throughput in the range of 3–9 kg/h, a barrel temperature in the range of 80–200°C and a rotation speed in the range of 120–300 rpm. The screw length is discretized according to the shortest length of an available screw element, that is, 15 mm. The available configurations of screw elements are in Table 4 and the characterization of the elements is given in Table 5. The feeding section is fixed and has screw elements with a high pitch of 30 mm to ensure that there is no back-flow to the feed port. The other elements can be freely arranged by the optimizer including screw mixing elements (SME), as well as conveying elements with different pitches and a left-handed element. The position of the alcohol feed can be varied to every discrete position within 20% and 80% of the overall extruder length.

Screw element type	A_1	A_2	σ_{BCM}
R30	0.5221	741	0
R20	0.3481	792	0
L20	−0.3481	792	0
SME (20)	0.3006	669	0.684

Note: A_1 is the screw conveying parameter, A_2 is the screw pressure parameter, and σ_{BCM} is the back-flow ratio for the elements with mass transport in both directions.[13,15]
Abbreviation: SME, screw mixing element.

TABLE 5 Flow and pressure characteristics of the different screw elements for the Leistritz 18 mm Maxx extruder.

Initial optimizations were carried out varying the alcohol feeding position, as well as the amount of alcohol fed as degrees of freedom for the optimizer and Equation (5) as cost function. The results showed that the optimal strategy to achieve the desired range for any target M_w is to not feed alcohol and by that to maximize the reaction rate given by Equation (1). The target M_w is in this case is controlled by the barrel temperature. Thereby the required residence time and, consequently, the specific energy demand are minimized. Although such operation would be theoretically possible, it violates the requirements for the product properties of commercial HEUR paint thickeners, as only a prepolymer is produced. To give the product the desired interaction in an aqueous solution, it has to be end capped by the alcohol

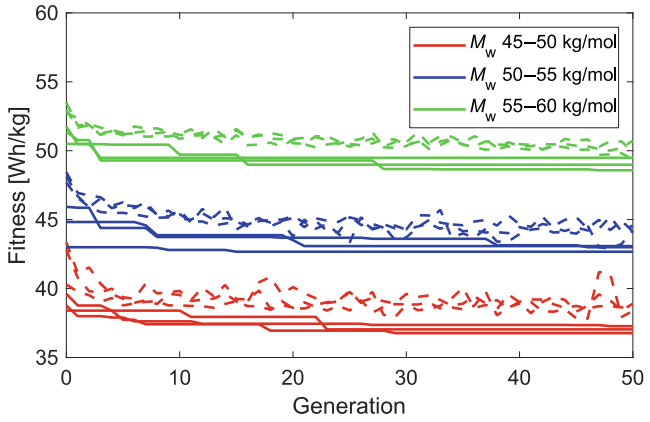

FIGURE 4 Convergence of the best values (solid) and mean (dashed) of the best 50% individuals of the population for each generation for different specifications of the molecular weight range for three runs of the memetic algorithm.

as shown in Figure 2. Therefore for the further optimizations, the alcohol feed was fixed to meet the stoichiometry of the target product composition at the various throughputs.

The convergence of the optimization is illustrated in Figure 4 for different runs over a total of 50 generations. The value of the best found individual of a generation is shown as well as the average value of the best 50% individuals of the population as a measure of the exploration of the search space of the optimizer. The optimization was repeated three times with different random seeds for the EA to quantify the influence the stochastic effects. Initially, fast improvements of the best solution are observed. This effect is caused by the combination of the EA with a local optimization for the continuous variables. With an increasing target molecular weight, more specific energy is required for the production process, as the product becomes more viscous. The main contributors to the quality of the solution are the position of the feed port of the alcohol along the extruder and the position of the restrictive left-handed element.

The high dependence of the process performance on the position of the left-handed element is exemplarily shown in Figure 5 for the target molecular weight range of 45–50 kg/mol. Figure 5 depicts all solutions that satisfy this constraint as a function of the position of the left-handed restrictive element. The positioning of the element at around 50 L/D shows the highest production efficiency. This position of the element provides the optimal location for the additional back pressure zone within the extruder and therefore provides the optimal residence time at the later stage of the reaction. Alternatively, the barrel temperature would have to be increased to achieve a similar reaction progress but with a lower energy efficiency.

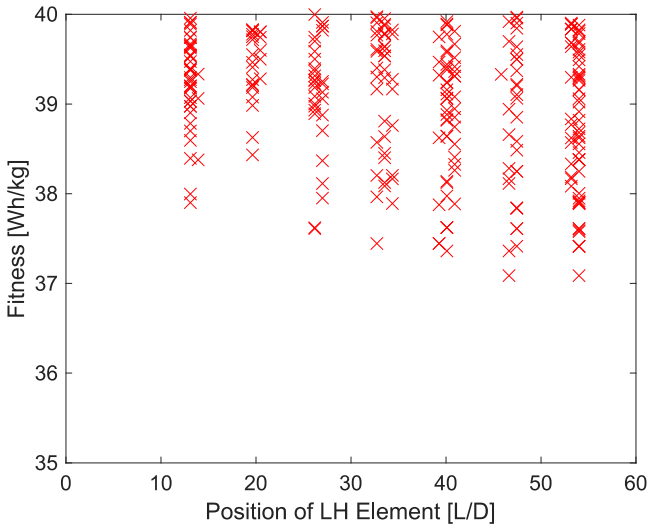

FIGURE 5 Scatter plot of the fitness as a function of the absolute position of the restrictive element for the M_w target range of 45–50 kg/mol.

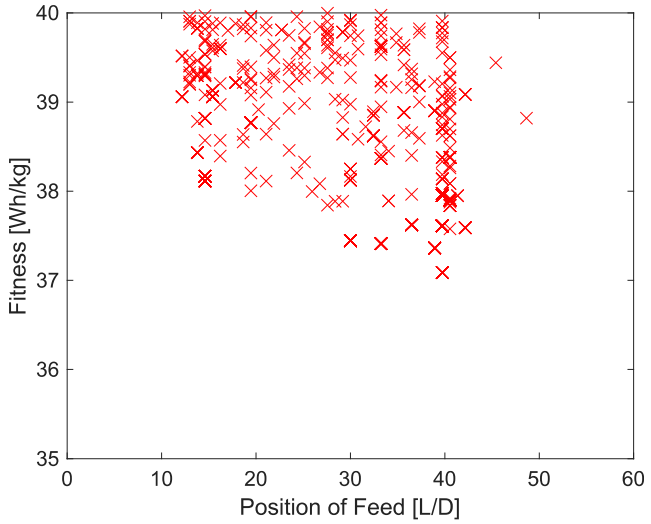

FIGURE 6 Scatter plot of the fitness as function of the position of the feed element of the alcohol for the M_w target range of 45–50 kg/mol.

Figure 6 shows the influence of the alcohol feed position on the process performance for the M_w range of 45–50 kg/mol. The sharp edge after around 40 L/D occurs as after a certain residence time, the degree of polymerization is close to the target molecular weight and further chain extension cannot be prevented. By overshooting the target molecular weight, more viscous dissipation is present in the melt, accelerating the chain growth further and consequently requiring a higher energy input for the process and leading to infeasible solutions. In direction of the feed, this effect be compensated by a lower barrel

Case	$\dot{m}$ (kg/h)	n (rpm)	$T_{b,1}$ (°C)	$T_{b,2}$ (°C)	Fitness (Wh/kg)
45–50	9.0	120.0	103.8	114.7	36.97
50–55	9.0	120.0	104.3	120.2	42.88
55–60	9.0	120.0	105.4	126.0	49.32

Abbreviation: HEUR, hydrophobically ethoxylated urethane.

TABLE 6 Optimal operating conditions for the HEUR case with cost function Equation (8) and an 18 mm extruder for different molecular weights.

temperature profile. As the reacted alcohol stops the chain growth reaction and leads to requiring more energy input, the alcohol feed should be located as close to the die as possible while satisfying the constraints.

Table 6 presents the optimal operating parameters for the HEUR process in the 18 mm extruder for the different cases. The optimal operation is at the upper bound of the throughput as sufficient residence time can be provided. For a higher throughput a safe and stable operation cannot be guaranteed as back flow and overloading of the feed may occur, especially for low speeds of rotation. The optimal rotation speed for all cases is at the lower bound. With a lower speed of rotation, a higher melt level is achieved in the extruder leading to a larger residence time, and also less mechanical energy is required. However, reducing the rotation speed further would lead to poor mixing of the reactants. A sufficient mixing especially of PEG and ISO is required as otherwise big deviations of the local stoichiometry may occur leading to a very broad distribution of molecular weights or to a highly cross-polymerized product that deposits on the screw elements. This is ensured in the optimization by the choice of the lower bound of the speed of rotation. The optimal barrel temperatures of both sections rise with increasing molecular weights as higher temperatures are required for a faster progress of the reaction for given residence times. As most of the residence time and mechanical dissipation are present in the later stage of the extruder due to the higher viscosity and the starved zone, the second barrel temperature is increased to satisfy the process constraints. Due to the higher activation energy of the chain growth compared with the chain termination, as given in Table 2, higher temperatures are preferred at the extruder die. The barrel temperatures in the first zone as well as the temperature difference between the zones even are increasing although this is penalized in Equation (8). The minimum specific energy input is increasing as the higher molecular weight product is more viscous and the production requires more residence time or more elevated temperatures. With a range of 35–50 Wh/kg product, the energy requirement is relatively low for extrusion applications. The typical range is from 50 Wh/kg for the processing of powder coating material to up to 250 Wh/kg for the industrial processing of polypropylene.[31] The high energy efficiency is caused by the late viscosity build-up in the extruder and the preheated liquid feeding of all reactants, avoiding the energy input for the heat of fusion. Experimental results on the Leistritz 18 mm Maxx with this HEUR system showed energy requirements of 350–650 Wh/kg depending on the operating conditions for throughputs between 2 and 3 kg/h. In the experimental results, the heating system is contributing 78% to the total energy demand whereas the motor is only contributing 22%. The 22% contribution of the motor includes a high base contribution of the friction, for example, in the gear-box and bearing, which cannot be neglected at low throughputs in practice. Additionally, the heating system of the extruder is not insulated to allow a maximal flexibility of the configuration. The heat losses to the environment of the 0.35 m^2 total barrel surface with a temperature difference of 100 K and an heat transfer coefficient of 25 W/(m^2K) between steel and air can be approximated to 843 W. For the investigated throughputs, this contributes 280–420 Wh/kg of the measured 300–500 Wh/kg for the majority of the required energy for heating. In combination, these two effects explain the difference between the simulation and the experimental results.

Figure 8 shows the screw designs for the optimal solutions in Table 6. As shown above, the location of the left-handed restrictive element is essential for the performance. With increasing specified molecular weight, the optimal position of this element shifts further towards the feeding section. This causes a longer starved zone and more residence time. Similarly, conveying elements with a lower pitch of 20 mm are located at later stages of the extruder. The position of the SME is moving towards the feed for more viscous products, providing more backmixing in the earlier stages of the extrusion process. These conclusions are supported by the simulation results of the optimal solutions shown in Figure 7. The profiles of the filling ratio over the length of the extruder show that with an increased target molecular weight, more residence time is provided towards the feed by the screw configurations, especially by the left-handed element. The pressure profiles indicate the location of the left-handed elements and the introduced back-pressure zones by pressure peaks. The die pressure is increasing up to 20 bar for the more viscous products. The elevated melt temperature profiles going up to 140°C do not

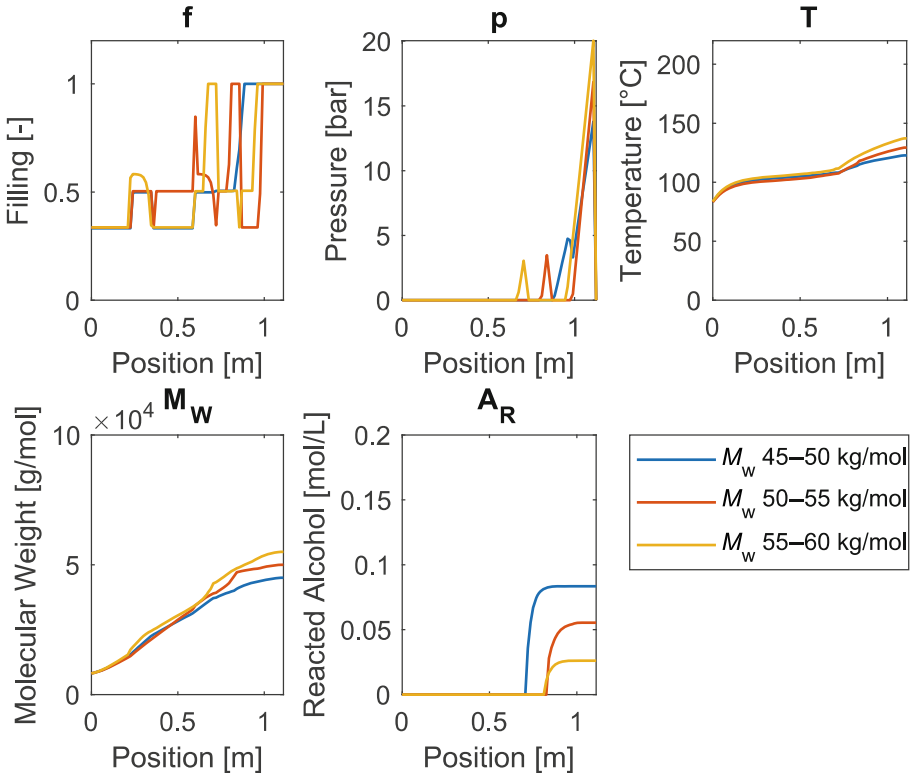

FIGURE 7 Simulation results for the filling rate, pressure, temperature, molecular weight, and concentration of the reacted alcohol for the best configurations for the different molecular weights. All variables are plotted over the axial position from the feed to the die within the extruder for the stationary case.

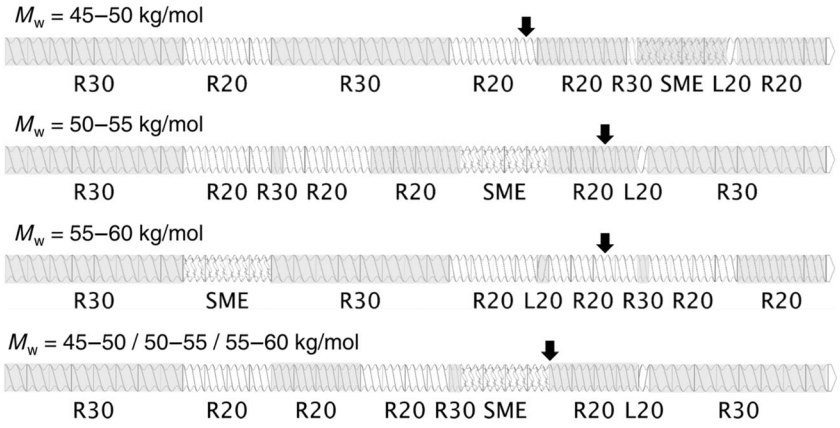

FIGURE 8 Optimal screw configurations for the different hydrophobically ethoxylated urethane products and the optimal combined configuration for the Leistritz 18 mm Maxx extruder. Indicated by the arrows are the feeding positions of the alcohol. SME, screw mixing element.

compensate the viscosity increase due to the higher molecular weight. A significant difference in the evolution of the molecular weight is observed in the last third of the reaction. In the case of a target molecular weight of 45–50 kg/mol, the alcohol is fed just before the starved zone, significantly reducing the further increase of the molecular weight. For the two higher target molecular weight ranges, the alcohol is fed at later positions. Due to the higher temperatures for the case of 55–60 kg/mol, the target molecular weight can still be achieved.

Comparing the optimal screw profiles for the different cases, similarities can be observed. Changing the screw configuration for every product would significantly reduce the flexibility as multiple sets of screws would have to be available on site and the pulling and replacing of the screws is much slower than the change of the operating conditions. This changeover time increases with the size of the extruders. Therefore the application of the same screw design for multiple products is desirable to increase the flexibility of the production. This optimization problem is tackled by simulating the extrusion process for all three products and summing up the fitness values of the three cases and minimizing the overall value.

The results of this optimization and of the previous ones are given in Table 7. C_1–C_3 represent the values of the cost function for the products for the individually optimized screw geometry and feeding position of the target case. The final row gives the result for the joint optimization of the configuration for all cases and adaptation

Case	C_1 (Wh/kg)	C_2 (Wh/kg)	C_3 (Wh/kg)	C_{total} (Wh/kg)
45–50	36.97	47.33	55.00	139.30
50–55	80.39	42.88	51.00	174.27
55–60	53.70	53.70	49.32	156.72
$\sum C_i$	39.17	45.49	51.00	135.65

Note: The columns give the cost function values of the optimized designs for the individual cases and their sum.

TABLE 7 Fitness of the optimal solutions for the different product requirements on the Leistritz 18 mm Maxx extruder with fixed designs and adapted operating conditions.

only of the operating parameters to the products to achieve the target molecular weight. The solution of the overall optimization problem is only up to 6% worse than the best individual solutions for each case and only 5% worse than the sum of all best individual solutions. In contrast, the individual best solutions are up to 30% worse in total performance over all three products. The corresponding optimal screw configuration for the production of all three HEUR grades is shown in Figure 8. The sequence of elements starting from the SME section to the die is identical to the optimal design for the middle target molecular weight of 50–55 kg/mol resulting in a good performance for the higher molecular weights. To increase the performance for the low-molecular weight product, the initial section is adjusted to provide more residence time in the first barrel section. So for the production of HEURs with different molecular weights, the application of a robust screw design for all products is the preferred alternative over using multiple screws or even multiple extruders.

TABLE 8 Flow and pressure characteristics of the screw elements for the Leistritz 27 mm Maxx extruder with a length of 30 mm (left) and the screw elements for the 75 mm Maxx extruder with a length of 60 mm.

27 mm elements	A_1	A_2	σ_{BCM}
R15	0.1655	844	0
R20	0.2207	827	0
R30	0.3310	794	0
R40	0.4414	761	0
L30	−0.3310	794	0
ZME 15	0.0513	73	0.04
75 mm elements	A_1	A_2	σ_{BCM}
R60	0.2837	820	0
R90	0.4255	784	0
R150	0.7091	711	0
L60	−0.2837	820	0

Note: A_1 is the screw conveying parameter, A_2 is the screw pressure parameter and σ_{BCM} is the back-flow ratio for the elements with mass-transport in both directions.[13,15]

3.2 | Optimization and scale-up of the HEUR production to an industrial scale extruder

The proposed model (Section 2.1) and optimization strategy (Section 2.3) were applied to up-scale to production extruders for the HEUR case study. For this investigation, the 27 mm extruder with L/D = 44 was chosen as a pilot scale equipment and two 75 mm extruders with L/D ratios of 40 and 60 were considered as the target production setup. The geometric parameters of the extruders are given in Table 1 and the parameters of the available screw elements can be seen in Table 8. All investigated extruders share geometric similarities as they have the same ratio between screw flight diameter and screw shaft, but this is not required for the application of the scale-up method.

The optimization of the 27 mm pilot scale extruder for the HEUR production was carried out similarly to the optimization of the 18 mm bench scale extruder with the goal to find the best screw configuration for the production of all three product grades. The discretization length was adjusted to 30 mm to account for the length of the larger screw elements. Figure 9 shows the resulting optimal screw design. Analogies to the screw design of the 18 mm extruder can be seen as the optimal position of the restrictive element is similar. Three tooth mixing element (ZME) provide an additional intense mixing just before the starved zone.

The optimal operating parameters for the pilot scale production are a throughput of 50 kg/h, a rotation speed of 180 rpm and barrel temperatures of 93, 97, and 100°C in the first section and 116, 129, and 140°C in the second section for the different products. The melt temperatures at the die for the three cases are 142, 156, and 169°C, they are significantly lower than the degradation temperatures of PEG and HEUR, which are above 200°C.[39] The higher temperatures of the barrel, compared with the 18 mm extruder, are required as the surface-to-volume ratio decreases with increasing extruder size. The viscosity of the product is sufficiently high so that enough

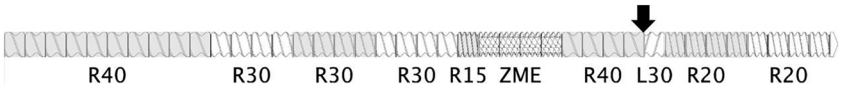

FIGURE 9 Optimal screw geometry for the Leistritz 27 mm Maxx extruder for the production of the three different hydrophobically ethoxylated urethane products. Indicated by the arrow is the feeding position of the alcohol.

TABLE 9 Optimal energy consumption for the different extruder sizes for the different HEUR products (C_1 = 45–50 kg/mol, C_2 = 50–55 kg/mol, and C_3 = 55–60 kg/mol).

Case	C_1 (Wh/kg)	C_2 (Wh/kg)	C_3 (Wh/kg)	C_{total} (Wh/kg)
18 mm Maxx	39.17	45.49	51.00	135.65
27 mm Maxx	44.92	52.12	60.55	157.59
75 mm Maxx	32.00	38.22	43.98	114.19
75 mm Maxx	27.85	33.41	38.70	99.96

Note: For all extruders, a single screw configuration and feeding position was optimized for all products, whereas the barrel temperatures, speeds of rotation, and throughputs were optimized for each product individually.
Abbreviation: HEUR, hydrophobically ethoxylated urethane.

mechanical energy can be introduced into the system to accelerate the reaction. Comparing the optimization results of the 27 mm extruder in Table 9 with the results of the 18 mm extruder, the energy requirement of the scaled-up extruder is about 15%–20% higher. This is caused by the increased melt temperature at the die for the 27 mm case. With scale-up, the contribution of the heat losses between the two barrel sections decreases as the throughput is increasing faster than the barrel size. If energy losses from the barrel to the environment were taken into account, which were not considered in this study, the efficiency of the larger extruder would improve in comparison to the smaller one.

The subsequent scale-up to the production level was performed for two extruders with a screw diameter of 75 mm and L/D ratios of 40 and 60 to analyze the influence of the extruder length on the optimal process design and operation. In contrast to the 18 and 27 mm extruders, no special mixing elements are included as these elements are rarely applied for larger equipment. The throughput was optimized in the range between 100 and 500 kg/h, the rotation speed in the range of 180–500 rpm and the barrel temperatures in the range of 80–160°C in the first barrel section and 80–200°C in the second barrel section. A speed of rotation of 180 rpm was the best operating condition for all 75 mm configurations, providing a good tradeoff between mixing and additional residence time. In case of L/D = 40, the most energy-efficient operating conditions are achieved at throughputs of 265, 242, and 229 kg/h with barrel temperatures of 155 and 160°C for the case of a molecular weight of 45 kg/mol and 160°C for all sections in the other two cases. For the case of L/D = 60, significantly higher throughputs of 489, 461, and 450 kg/h were found to be optimal with barrel temperatures of 120°C in the first section and 130°C in the second section. Overall as shown in Table 9, the efficiency was increased by 16% for L/D = 40 in case of the 75 mm extruder compared with L/D = 60 of the 18 mm extruder. By choosing the 75 mm extruder with L/D = 60, the specific energy consumption can further be reduced by 13%, while almost doubling the throughput. Higher heat losses to the environment caused by the extended extruder length can be neglected because of the good insulation of the extruder barrel. The primary factor that contributes to reducing the specific energy consumption is the increased contribution of shear-induced heating, while the heating of the barrel has a negative impact. The input of mechanical energy by the motor is therefore more efficient, which is in

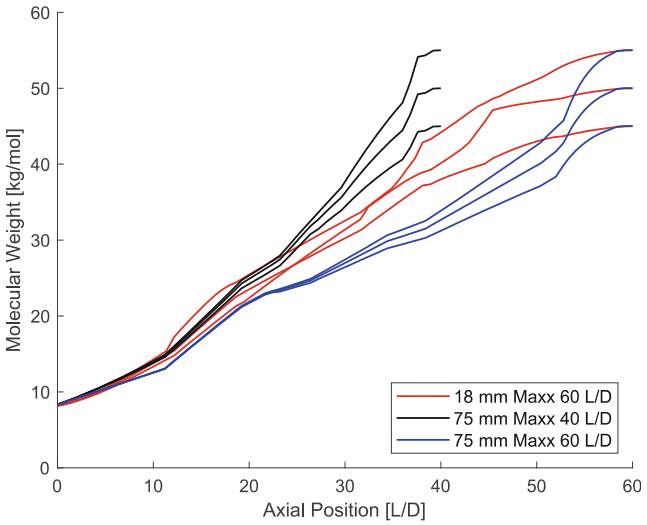

FIGURE 10 Evolution of the molecular weight over the length of the extruder for the different extruder sizes and the three different target molecular weights.

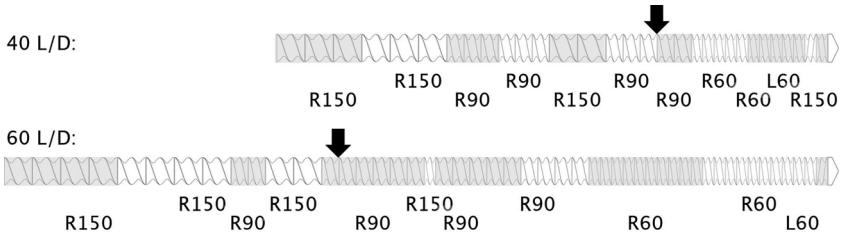

FIGURE 11 Optimal screw geometry for the Leistritz 75 mm Maxx extruder for the production of the different products. Indicated by the arrows are the feeding positions of the alcohol.

agreement with the general scale-up of extruders, where the contribution of the heating and cooling elements relative to the mechanical input is decreasing towards larger equipment sizes. This is caused by the increase of volume-to-surface ratio for larger extruders. Furthermore, the increase of the molecular weight happens later, resulting in a smaller portion of energy introduced in the part where the reaction was completed. This can be seen in Figure 10. Additionally, lower barrel temperatures were sufficient due to the longer mean residence time of about 40 s for the L/D = 60 extruder compared with the shorter residence time of 17 s for L/D = 40. These differences in the optimal evolutions emphasize that a simple scale-up strategy is not always applicable in the design of reactive extrusion processes. The different availability of screw elements for different extruder sizes can be handled easily by the model and the optimization-based scale-up approach.

The optimal screw designs for the 75 mm extruder with L/D = 40 and L/D = 60 are shown in Figure 11. The restrictive element with 60 mm pitch (L60) is placed as far as possible towards the die. Furthermore, the positions of the low pitch elements (R60) towards the die and the high pitch elements (R150, R90) in the feeding zone indicate that the optimal configuration is to maximize the residence time in the later reaction zone, after the addition of the alcohol at 28 L/D (L/D = 40) and 16 L/D (L/D = 60). Overall the optimization results show that an energetically efficient process can be performed at industrially relevant throughputs of about 500 kg/h on a 75 mm extruder with a L/D = 60.

4 | DISCUSSION

4.1 | Optimization

The results of the optimization of the 18 mm bench scale extruder in Section 3.1 and for the scale-up in Section 3.2 demonstrate the potential for flexible and energetically efficient use of extruders for the production of HEUR grades with different molecular weights. In the current industrial practice, HEURs are produced in batches of several cubic meters. The HEUR systems are highly viscous and therefore during the batch reaction and the subsequent formulation in water, a large energy input by the stirrer is required over long periods of time. Production times for the batch process are typically in the range of 1–4 h with energy inputs of 1000–5000 Wh/kg. In contrast, the reactive extrusion process offers a significantly better energy efficiency in the range of 27–60 Wh/kg, as the overall residence time is much shorter due to higher temperatures and more efficient local mixing. The experimental study on the 18 mm extruder showed similar rheological properties of the melt and of the final aqueous solution compared with the product produced in batch. By transition from the batch process to the reactive extrusion process, the tedious cleaning step after each charge can be omitted and the product can be further processed as a solid. Moreover, the quantity of the processed hazardous diisocyanates at a given location is significantly reduced in the reactive extrusion approach compared with a charge of a conventional reactor, due to their significant difference in the volume. In practice, the hold-up within the extruder is around 100 times smaller than in a batch production with a similar production capacity. Additionally, in the batch production, the maximum achievable product viscosity, batch size, and the production rate per vessel are constrained by the power of the stirrer. The usual melt viscosities of the HEUR product, in the range of 400–800 Pa s at 100°C, are at the lower bound of the operating window of a typical extrusion process and an easy scale-up to higher throughputs is possible by the choice of larger extruders. Even for the scale-up of the extruders to production capacities of almost 500 kg/h using the 75 mm extruder with L/D = 60, the equipment footprint remains small compared with batch reactors.

This throughput corresponds to the production of almost 1000 t/year for a 1 shift production per machine. The presented model addresses all process-relevant effects independent of the extruder size and enables a rigorous model-based scale-up and optimization. The results are very promising. All process constraints are satisfied and the most beneficial process configuration was determined. The use of the same reaction model and property data as for the smaller equipment leads to a very fast and transparent scale-up, as all process states are available

from the simulation. The availability of this data source in the model-based scale-up enables a more time- and cost-efficient scale-up in reactive extrusion as experimental trials can be reduced to a minimum with accurate predictions of the process performance and product quality.

4.2 | Dynamic process operation

In Section 3, we showed that the efficient continuous production of different HEUR products on the same extruder is possible. The current industrial practice is a pure batch production with the flexibility to change the product grade only between the charges. We also discuss the dynamic operation of the continuous reactive extrusion process particular with respect to product changeovers. If a similar flexibility can be achieved with the reactive extrusion production, the existing logistics, procurement, distribution, and shift planning structure can be used. Necessary changes in this existing structure otherwise may result in costs that dominate the savings from the process improvement.[40,41] Therefore in the following, the dynamic product changeover between two different HEUR grades is investigated.

Simulations of a product changeover between two material grades in the continuous extrusion process for the 18 mm Maxx extruder are shown in Figure 12 and emphasize the flexibility of the new production concept, as a product changeover can be performed within 300 s. In Figure 12, the melt temperature and the molecular weight M_w at the die are shown for product changeovers to a product with a higher and with a lower viscosity.

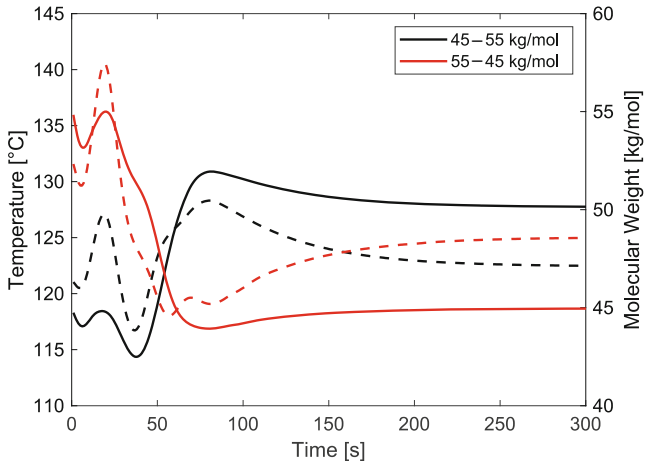

FIGURE 12 Simulation of product changeovers between the two optimal operating conditions on the Leistritz 18 mm Maxx extruder for changeovers between products of 45 and 55 kg/mol. The dashed lines indicate the temperature and the solid lines indicate the evolution of the molecular weight at the die.

At the throughput of 9 kg/h on the 18 mm extruder the mean residence time is around 85 s. This simulation model considers the thermal inertia of the barrel temperature for changeover, assuming a ramp for the barrel temperatures. For the 18 mm extruder, experiments on the real equipment showed transition times of 50 s for a 10 K temperature increase and 35 s for a decrease of the barrel temperature by 10 K. The evolution of the molecular weight in the early stage of the reaction is similar for the different products as shown in Figure 7. The end-capping in the later extruder section determines the quality of the product and primarily contributes to the changeover time. Therefore, product changeovers are possible within the order of magnitude of one residence time. We expect a similar performance for product changeovers for the 27 and 75 mm extruders as the mean residence times and the thermal inertia of the extruders are in the same range. Finally, the continuous production enables a direct reaction to process deviations mitigating the risk of producing an entire off spec charge as in the case of problems in batch production.

5 | CONCLUSIONS

In this article, we applied the detailed mechanistic reactive extrusion model and the flexible and broadly applicable memetic optimization method for the design and optimization of the processing conditions from Ref. 13 to the industrial production of HEUR paint thickeners. The results of the optimization demonstrate the potential of the reactive extrusion process as a cost-effective and environmentally favorable alternative to the conventional batch production. The transition from a batch reactor to an extruder offers the possibility to significantly reduce the energy consumption of the manufacturing process by up to 90% and enables the production of new high-molecular weight products. The outcomes of the simulation and optimization show that it is possible to produce HEUR grades with different molecular weights using a single screw configuration. This approach can be applied with only a minimal deviation from the established optimal parameters, causing <5% loss of energy efficiency compared with using tailored configurations that were specifically optimized for each target molecular weight. Model-based scale-up was investigated for the same products in four increasing sizes of the extruder and the Leistritz 75 mm Maxx extruder with L/D = 60 was identified as the most suitable equipment for an industrial production rate of 500 kg/h. The proposed model-based optimization and scale-up are reliable and transparent, as all relevant process quantities are accessible from the simulation and the optimal configurations can be analyzed in

detail. Moreover, the dynamic simulations of the product changeover showed the feasibility to switch between the product grades within 300 s, ensuring minimal material losses and offering the option for in-process troubleshooting which is unattainable in the conventional batch operations. This flexibility of the reactive extruder makes it possible to produce amounts that differ from multiples of a full batch in the conventional production, which is particularly relevant in the market of specialty additives. The use of this increased flexibility will be further investigated in future work on the application of demand-side management strategies[42] to react dynamically to the varying availability and price of electricity. Finally, a combination of measured process data and the process model described here can be employed for improved process control of reactive extrusion processes.[43]

ACKNOWLEDGMENTS

This research was funded by the European Union's Horizon 2020 research and innovation program under grant agreement no. 820716 SIMPLIFY. (http://www.spire2030.eu/simplify). Emina Kurtovic and Christian Backhaus are kindly acknowledged for their contribution to the laboratory experiments. Open Access funding enabled and organized by Projekt DEAL.

CONFLICT OF INTEREST STATEMENT

The authors declare no potential conflict of interest.

DATA AVAILABILITY STATEMENT

The presented data of this study are available from the corresponding author upon reasonable request.

ORCID

Maximilian Cegla https://orcid.org/0000-0002-0830-8603

Sebastian Engell https://orcid.org/0000-0002-3125-9846

REFERENCES

1. Kutsch O. Market analysis paintings and coatings. 2022.
2. Eley RR. Applied rheology in the protective and decorative coatings industry. *Rheol Rev*. 2005;3:173-240.
3. Bieleman J. *Additives for coatings*. Wiley; 2000. doi:10.1002/9783527613304
4. Quienne B, Pinaud J, Robin J-J, Caillol S. From architectures to cutting-edge properties, the blooming world of hydrophobically modified ethoxylated urethanes (HEURs). *Macromolecules*. 2020;53(16):6754-6766. doi:10.1021/acs.macromol.0c01353
5. Reuvers AJ. Control of rheology of water-borne paints using associative thickeners. *Prog Org Coatings*. 1999;35(1–4):171-181. doi:10.1016/S0300-9440(99)00014-4
6. May R, Kaczmarski JP, Glass JE. Influence of molecular weight distributions on HEUR aqueous solution rheology. *Macromolecules*. 1996;29(13):4745-4753. doi:10.1021/ma9507655
7. SIMPLIFY. Sonication and microwave processing of material feedstock. https://www.aspire2050.eu/simplify
8. Bampouli A, Tzortzi I, de Schutter A, et al. Insight into Solventless production of hydrophobically modified ethoxylated urethanes (HEURs): the role of moisture concentration, reaction temperature, and mixing efficiency. *ACS Omega*. 2022;7:36567-36578. doi:10.1021/acsomega.2c04530
9. Cegla M, Engell S. Application of real-time optimization with modifier adaptation to the reactive extrusion of hydrophobically modified ethoxylated urethanes. In: Montastruc L, Negny S, eds. *Computer Aided Chemical Engineering*. Vol 51. Elsevier B.V. 2022:1189-1194. doi:10.1016/B978-0-323-95879-0.50199-5
10. Cegla M, Engell S. Generation-aware electrified production: optimal continuous industrial production of paint thickeners. *Chem Eng Trans*. 2022;96(June):31-36. doi:10.3303/CET2296006
11. Wołosz D, Fage AM, Parzuchowski PG, Świderska A, Brüll R, Elsner P. Sustainable associative thickeners based on hydrophobically modified ethoxylated poly(hydroxy-urethane)s end-capped by long alkyl chains. *Prog Org Coatings*. 2023;179:107514. doi:10.1016/j.porgcoat.2023.107514
12. Wołosz D, Fage AM, Parzuchowski PG, Świderska A, Brüll R. Reactive extrusion synthesis of biobased isocyanate-free hydrophobically modified ethoxylated urethanes with pendant hydrophobic groups. *ACS Sustain Chem Eng*. 2022;10(35):11627-11640. doi:10.1021/acssuschemeng.2c03535
13. Cegla M, Engell S. Optimal design and operation of reactive extrusion processes: Modelling, model validation and optimization algorithm. *Polym Eng Sci*. 2023;63(12):4153-4173. doi:10.1002/pen.26515
14. Bhavsar RA, Nehete KM. Rheological approach to select most suitable associative thickener for water-based polymer dispersions and paints. *J Coatings Technol Res*. 2019;16(4):1089-1098. doi:10.1007/s11998-019-00194-6
15. Eitzlmayr A, Koscher G, Reynolds G, et al. Mechanistic modeling of modular co-rotating twin-screw extruders. *Int J Pharm*. 2014;474(1–2):157-176. doi:10.1016/j.ijpharm.2014.08.005
16. Wesholowski J, Hoppe K, Nickel K, Muehlenfeld C, Thommes M. Scale-up of pharmaceutical hot-melt-extrusion: process optimization and transfer. *Eur J Pharm Biopharm*. 2019;142(January):396-404. doi:10.1016/j.ejpb.2019.07.009
17. Gottschalk T, Özbay C, Feuerbach T, Thommes M. Predicting throughput and melt temperature in pharmaceutical hot melt extrusion. *Pharmaceutics*. 2022;14(9):1757. doi:10.3390/pharmaceutics14091757
18. Berzin F, David C, Vergnes B. Optimization and scale-up of twin-screw reactive extrusion: the case of EVA transesterification. *Int Polym Process*. 2020;35(5):422-428. doi:10.3139/217.3958
19. Eitzlmayr A, Khinast J, Hörl G, et al. Experimental characterization and modeling of twin-screw extruder elements for pharmaceutical hot melt extrusion. *AIChE J*. 2013;59(11):4440-4450. doi:10.1002/aic.14184
20. Cegla M, Engell S. Reliable modelling of twin-screw extruders by integrating the backflow cell methodology into a mechanistic model. *Computer Aided Chemical Engineering*. Vol 48. Elsevier; 2020:175-180. doi:10.1016/B978-0-12-823377-1.50030-6
21. Barmar M, Barikani M, Kaffashi B. Synthesis of ethoxylated urethane and modification with cetyl alcohol as thickener. *Iran Polym J*. 2001;10(5):331-335.

22. Verhoeven VWA, Van Vondel MPY, Ganzeveld KJ, Janssen LPBM. Rheo-kinetic measurement of thermoplastic polyurethane polymerization in a measurement kneader. *Polym Eng Sci*. 2004;44(9):1648-1655. doi:10.1002/pen.20163
23. Cassagnau P, Nietsch T, Michel A. Bulk and dispersed phase polymerization of urethane in twin screw extruders. *Int Polym Process*. 1999;14(2):144-151. doi:10.3139/217.1531
24. Odian G. Step polymerization. *Principles of Polymerization*. John Wiley and Sons, Inc.; 2004:39-197.
25. Cassagnau P, Nietsch T, Bert M, Michel A. Reactive blending by in situ polymerization of the dispersed phase. *Polymer*. 1998; 40(1):131-138. doi:10.1016/S0032-3861(98)00210-9
26. Clariant International AG. Polyglykol product brochure. 2020 http://www.essentialingredients.com/pdf/PolyglykolsforPersonalCare.pdf
27. Gaspar-Cunha A, Covas JA, Vergnes B. Defining the configuration of co-rotating twin-screw extruders with multiobjective evolutionary algorithms. *Polym Eng Sci*. 2005;45(8):1159-1173. doi:10.1002/pen.20391
28. Teixeira C, Covas JA, Stützle T, Gaspar-Cunha A. Multi-objective ant colony optimization for the twin-screw configuration problem. *Eng Optim*. 2012;44(3):351-371. doi:10.1080/0305215X.2011.639370
29. Teixeira C, Covas JA, Berzin F, Vergnes B, Gaspar-Cunha A. Application of evolutionary algorithms to the definition of the optimal twin-screw extruder configuration for starch cationization. *Polym Eng Sci*. 2011;51(2):330-340. doi:10.1002/pen.21801
30. Teixeira C, Covas J, Stützle T, Gaspar-Cunha A. Hybrid algorithms for the twin-screw extrusion configuration problem. *Appl Soft Comput J*. 2014;23:298-307. doi:10.1016/j.asoc.2014.06.022
31. Kohlgrüber K. *Co-Rotating Twin-Screw Extruder Fundamentals, Technology, and Applications*. Carl Hanser Verlag GmbH & Co KG; 2008.
32. Fukuda G, Chavez D, Bigio DI, Wetzel M, Andersen P. Investigation of scale-up methodologies in twin-screw compounding. *Annu Techn Conf – ANTEC Conf Proc*. 2014;2(January):1142-1150.
33. Potente H. Existing scale-up rules for single-screw Plasticating extruders. *Int Polym Process*. 1991;6(4):267-278. doi:10.3139/217.910267
34. Nakatani M. Scale-up theory for twin-screw extruder, keeping the resin temperature unchanged. *Adv Polym Technol*. 1998; 17(1):19-22.
35. Nastaj A, Wilczyński K. Optimization and scale-up for polymer extrusion. *Polymers*. 2021;13(10):1547. doi:10.3390/polym13101547
36. Ortiz-Rodriguez E, Tzoganakis C. Scaling-up a reactive extrusion operation: a one-dimensional simulation analysis. *Int Polym Process*. 2010;25(3):242-250. doi:10.3139/217.2346
37. Nauman EB. Nonisothermal reactors. Theory and application of thermal time distributions. *Chem Eng Sci*. 1977;32(4):359-367. doi:10.1016/0009-2509(77)85002-1
38. Pradel JL, David C, Quinebèche S, Blondel P. Scale up tools in reactive extrusion and compounding processes. Could 1D-computer modeling be helpful? *AIP Conf Proc*. 2014;1593-(February):530-533. doi:10.1063/1.4873837
39. Athanasoulia IG, Tarantili PA. Preparation and characterization of polyethylene glycol/poly(L-lactic acid) blends. *Pure Appl Chem*. 2017;89(1):141-152. doi:10.1515/pac-2016-0919
40. Gu J, Goetschalckx M, McGinnis LF. Research on warehouse operation: a comprehensive review. *Eur J Oper Res*. 2007; 177(1):1-21. doi:10.1016/j.ejor.2006.02.025
41. van Heeswijk W, Mes M, Schutten M. In: Zijm H, Klumpp M, Regattieri A, Heragu S, eds. *Operations, Logistics and Supply Chain Management*. Springer International Publishing; 2019. doi:10.1007/978-3-319-92447-2
42. Cegla M, Semrau R, Tamagnini F, Engell S. Flexible process operation for electrified chemical plants. *Curr Opin Chem Eng*. 2023;39:100898. doi:10.1016/j.coche.2023.100898
43. Cegla M, Fage A, Kemmerling S, Engell S. Proceedings of the IFAC World Congress 2023 Yokohama - IFAC-papers online series. Experimental application of real-time optimization with modifier adaptation and quadratic approximation to a reactive extrusion process. (Accepted) IFAC WC 2023 – IFAC-Papers Online. Elsevier; 2023.

How to cite this article: Cegla M, Fage A, Kemmerling S, Engell S. Optimal design and operation of reactive extrusion processes: Application to the production and scale-up of polyurethane rheology modifiers for paints. *Polym Eng Sci*. 2023;63(12):4220-4235. doi:10.1002/pen.26519